



# CoBP nanoparticles supported on three-dimensional nitrogen-doped graphene hydrogel and their superior catalysis for hydrogen generation from hydrolysis of ammonia borane

Yana Men <sup>a,1</sup>, Jun Su <sup>b,1</sup>, Xiaoqiong Du <sup>a</sup>, Lijing Liang <sup>a</sup>, Gongzhen Cheng <sup>a</sup>, Wei Luo <sup>a,\*</sup>

<sup>a</sup> College of Chemistry and Molecular Sciences, Wuhan University, Wuhan, Hubei, 430072, PR China

<sup>b</sup> Wuhan National Laboratory for Optoelectronics, Huazhong University of Science and Technology, Wuhan, Hubei, 430074, PR China

## ARTICLE INFO

### Article history:

Received 20 September 2017

Received in revised form

1 November 2017

Accepted 10 November 2017

Available online 11 November 2017

### Keywords:

Nitrogen-doped graphene hydrogel

CoBP

Hydrogen storage

Ammonia borane

## ABSTRACT

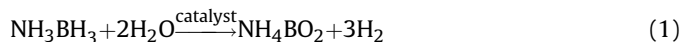
P-doped noble-metal-free CoB nanoparticles (NPs) anchored on a three-dimensional nitrogen-doped graphene hydrogel (NGH) have been successfully synthesized through a simple one-pot co-reduction method and further used as catalyst toward catalytic hydrolysis of ammonia borane (NH<sub>3</sub>BH<sub>3</sub>) at room temperature. Benefiting from the synergistic electronic effect between Co, B, and P, as well as the strong metal-support interaction between CoBP and 3D NGH, the as-synthesized Co<sub>0.79</sub>B<sub>0.15</sub>P<sub>0.06</sub>/NGH catalyst exhibits excellent catalytic activity toward hydrolysis of ammonia borane, with the turnover (TOF) value of 32.8 min<sup>-1</sup>, which is almost 5 times higher than that of undoped Co<sub>0.85</sub>B<sub>0.15</sub>/NGH NPs, and higher than most of the reported noble metal free catalysts.

© 2017 Elsevier B.V. All rights reserved.

## 1. Introduction

Hydrogen has been considered as one of the most promising alternative energy carrier for the future energy conversion and storage, probably due to its high energy density and environmental benignity [1–6]. However, safe and efficient storage of hydrogen still remains a key issue to the forthcoming “hydrogen economy” [7–9]. To this end, a large number of hydrogen storage approaches have been investigated, including physical absorption materials [10,11], metal hydrides [12,13], and chemical hydrides [14–16]. Among them, ammonia borane (NH<sub>3</sub>BH<sub>3</sub>, AB) with high stability and high hydrogen content (19.6 wt.%) [17–20], has been considered as the most potential candidate for the chemical hydrogen storage material [21–25]. As shown in Eq. (1), AB is able to release hydrogen through the catalytic hydrolysis process, in which 3 mol H<sub>2</sub> can be obtained [26]. Currently, noble metal based materials (Rh, Pt, or Ru) [27–30] are considered as the most effective catalysts for catalytic hydrolysis of ammonia borane, however, their high cost and scarcity severely hinder their large-scale applications. Therefore, the development of noble-metal-free, highly efficient and

sustained catalysts toward hydrolysis of AB is extremely desirable, but still a great challenge [31,32].



Hetero-atoms doping has been considered as one of the most efficient way to increase the catalytic activity of metal catalysts. Transition metal phosphides (TMPs), which have a slight of charge transfer from the metal atoms to P [33–35], have been extensively served as effective electrocatalysts in overall water splitting [36–41], on account of a strong electronic interaction between the metal and P. Recently, Fu and coworkers first reported Ni<sub>2</sub>P Nanocatalysts prepared by reacting Ni(OH)<sub>2</sub> powder with solid NaH<sub>2</sub>PO<sub>2</sub> in argon at 543 K and their excellent catalytic performance in the dehydrogenation of AB [42]. Subsequently, the same group reported CoP nanoparticles obtained from a Co precursor using the NaH<sub>2</sub>PO<sub>2</sub>-reduction method in argon at 573 K toward effectively catalytic hydrolysis of AB [43]. On the other hand, transition metal borides, such as CoB, NiB, and Co-Ni-B have already shown great potential as catalysts toward catalytic hydrolysis of AB [44–46]. Despite great efforts have been made, it still remains a big challenge to achieve desired non-noble metal based catalysts with high efficiency and long-term stability. Moreover, to the best of knowledge, doping two hetero-atoms into non-noble metal-based catalyst with

\* Corresponding author.

E-mail address: [wluo@whu.edu.cn](mailto:wluo@whu.edu.cn) (W. Luo).

<sup>1</sup> These authors contributed equally.

enhanced catalytic activity toward catalytic hydrolysis of AB, has not been reported yet.

Following this strategy, herein, for the first time, we reported a simple one-pot synthesis of CoBP nanoparticles (NPs) supported on three dimensional (3D) nitrogen-doped graphene hydrogel (NGH), and their superior catalytic performance toward catalytic hydrolysis of AB. The 3D NGH was chosen as the supported substrate for arching the as-synthesized CoBP NPs due to its large surface area, porosity, electrical conductivity, and excellent stability [47–50]. Thanks to the synergistic electronic interaction between Co, B, and P, as well as the strong metal-support interaction between CoBP and 3D NGH, the obtained  $\text{Co}_{0.79}\text{B}_{0.15}\text{P}_{0.06}/\text{NGH}$  exhibits superior catalytic performance toward hydrolysis of AB, with a turnover frequency value (TOF) of  $32.8 \text{ min}^{-1}$ , which is higher than most of the reported non-noble metal based catalysts, and even comparable to noble metal based catalysts.

## 2. Experimental

### 2.1. Chemicals and materials

All chemicals were commercial and used without further purification. Ultrapure water was used as the reaction solvent.

Cobalt chloride hexahydrate ( $\text{CoCl}_2 \cdot 6\text{H}_2\text{O}$ , Sinopharm Chemical Reagent Co., Ltd.,  $\geq 99\%$ ), Sodium hypophosphite ( $\text{NaH}_2\text{PO}_2$ , Aladdin Co., Ltd.  $\geq 99.0\%$ ), Sodium ammonia sulfate ( $(\text{NH}_4)_2\text{SO}_4$ , Aladdin Co., Ltd.  $\geq 99.0\%$ ) Tetrahydrofuran (THF, Sinopharm Chemical Reagent Co., Ltd.,  $> 98\%$ ), sodium borohydride ( $\text{NaBH}_4$ , Sinopharm Chemical Reagent Co., Ltd.,  $> 96\%$ ), potassium permanganate ( $\text{KMnO}_4$ , Shanghai Chemic Co., Ltd,  $\geq 99.5\%$ ), hydrogen peroxide ( $\text{H}_2\text{O}_2$ , Sinopharm Chemical Reagent Co., Ltd,  $\geq 30\%$ ), phosphoric acid ( $\text{H}_3\text{PO}_4$ , Sinopharm Chemical Reagent Co., Ltd, AR), sulfuric acid ( $\text{H}_2\text{SO}_4$ , Sinopharm Chemical Reagent Co., Ltd, 95–98%), ethanol absolute ( $\text{C}_2\text{H}_5\text{OH}$ , Sinopharm Chemical Reagent Co., Ltd.,  $\geq 99.7\%$ ), ethylenediamine ( $\text{C}_2\text{H}_8\text{N}_2$ , Sinopharm Chemical Reagent Co., Ltd.,  $\geq 99.0\%$ ), graphite power (Sinopharm Chemical Reagent Co., Ltd,  $\geq 99.85\%$ ) were used as received.

### 2.2. Preparation of ammonia borane (AB)

Sodium borohydride ( $\text{NaBH}_4$ , 0.05 mol) and sodium ammonia sulfate ( $(\text{NH}_4)_2\text{SO}_4$ , 0.1 mol) were added to a 250 mL two-necked round-bottom flask with one neck connected to a condenser. Tetrahydrofuran (THF, 100 mL) was transferred into the flask, and the contents were vigorously stirred at 313 K. The reaction was under a nitrogen atmosphere. After 4 h, the resultant solution was filtered by suction filtration and the filtrate was concentrated under vacuum at room temperature. Then, the product was purified by diethyl ether.

### 2.3. Preparation of graphene oxide (GO)

(Graphene oxide) GO was prepared by a modified Hummers method [51]. During this process, 3.0 g carbon black was added into a mixture of concentrated  $\text{H}_2\text{SO}_4/\text{H}_3\text{PO}_4$  (360:40 mL) in a 1 L flask. Then, a certain amount of  $\text{KMnO}_4$  (18.0 g) was gradually added to the flakes. The resulting mixture was then heated to 323 K and stirred for 12 h. After cooling to room temperature, the mixture was added to 400 mL of water with 30%  $\text{H}_2\text{O}_2$  (3 mL). After adding 2 mL of excess  $\text{H}_2\text{O}_2$ , a permanent yellow color was formed, which indicated that the complete oxidation of the graphite was observed. The resulting solution was centrifuged to obtain the product. Then, the obtained product was washed with deionized water, 30% diluted hydrochloric acid, and absolute ethyl alcohol many times and then dried in vacuum at 298 K.

### 2.4. Preparation of N-doped graphene

During a typical synthesis of the N-doped graphene (NGH) process, 630 mg of GO was added into a 100 mL flakes with 70 mL of deionized water. A GO dispersion of 9 mg/mL was obtained by ultrasonication for 2 h, which was doped with nitrogen (N) atoms by adding 3.0 mL of  $\text{C}_2\text{H}_8\text{N}_2$  gradually at room temperature. In the next step, the suspension was stirred magnetically at 298 K for 30 min and subsequently transferred into a 100 mL Teflon-lined autoclave which was heated at 180 °C for 12 h. After being cooled to room temperature, the as-obtained NGH hydrogel was dialyzed against DI-water for at least 24 h to remove the impurities.

### 2.5. Synthesis of CoBP/NGH catalysts

In a typical experiment for CoBP/NGH NPs, 4 mg NGH was dispersed into 1.5 mL ultrapure water in a two-necked round bottom flask. The mixture was dispersed uniformly by ultrasonication. Then, 0.4 mL cobalt chloride solution ( $\text{CoCl}_2$ , 0.1 mol  $\text{L}^{-1}$ ), and different amounts of  $\text{NaH}_2\text{PO}_2$  solution (0 mmol, 0.02 mmol, 0.06 mmol, 0.1 mmol, 0.1 mol  $\text{L}^{-1}$ ) were added into the flask. Ultrasonication was required to obtain an equally dispersion. The resulting mixture was then reduced by aqueous solution containing 1 mmol  $\text{NaBH}_4$  with vigorous stirring at 298 K. After the reaction completely, the product was collected by centrifugation washing, and drying by pump vacuum.

### 2.6. Catalytic hydrolysis of AB

In a typical experiment, The hydrolysis reaction of AB by CoBP/NGH NPs were tested at 298 K. Various CoBP/NGH NPs doping with different phosphorus content were added into a 25 mL two-necked round bottom flask. One neck was connected to a gas burette to monitor the volume of the gas evolution, and the other for the introduction of AB (1 mmol, 1 mol  $\text{L}^{-1}$ ). A water bath was used to control the temperature of the reaction solution at 298 K. The value of turnover frequency (TOF) can be calculated using Equation (2).

$$\text{TOF}_{\text{initial}} = \frac{P_{\text{atm}} V_{\text{H}_2} / RT}{n_{\text{Co}} t} \quad (2)$$

where TOF initial is initial turnover frequency,  $P_{\text{atm}}$  is the atmospheric pressure,  $V_{\text{H}_2}$  is the volume of the generated gas when the conversion reached 50%,  $R$  is the universal gas constant,  $T$  is room temperature (298 K),  $n_{\text{Co}}$  is the mole amount of Co and  $t$  is the reaction time. The temperatures were varied from 298 to 313 K to obtain the activation energy ( $E_a$ ), while CoBP/NGH and AB were kept the same ratio (catalyst/AB = 0.04).

### 2.7. Cycle stability tests

For cycle stability tests, catalytic reactions were tested 5 times by adding another the same molar contents of AB (1 mmol) after the previous cycle at 298 K.

### 2.8. Physical characterizations

Powder X-ray diffraction (XRD) patterns were measured by a Bruker D8-Advance X-ray diffractometer using  $\text{Cu K}\alpha$  radiation source ( $\lambda = 0.154178 \text{ nm}$ ) with a velocity of  $8^\circ/\text{min}$ . Inductively coupled plasma-atomic emission spectroscopy (ICP-AES) was performed on IRIS Intrepid II XSP. X-ray photoelectron spectroscopy (XPS) measurement was performed with a Kratos XSAM 800 spectrophotometer. The morphologies and sizes of the samples were observed by Tecnai G20 U-Twin transmission electron

microscope (TEM) equipped with an energy dispersive X-ray detector (EDX) at an acceleration voltage of 200 kV. Scanning electron microscopy (SEM) images were obtained using an electron microscope (SIGMA, ZEISS).

### 3. Results and discussion

Nitrogen-doped graphene hydrogel (NGH) was first prepared at 180 °C according to a reported hydrothermal method [52]. Then the CoBP/NGH catalysts with different phosphorus doping were successfully prepared via a simple one-pot co-reduction approach and studied for catalytic hydrogen generation toward hydrolysis of AB at room temperature. During this process, the NGH was used as support. NaBH<sub>4</sub> was not only used as a boron source, but also as a reductant, in which the metal precursors were reduced to form CoB NPs. The CoBP/NGH with different phosphorus doping were obtained by changing the amounts of NaH<sub>2</sub>PO<sub>2</sub>, which were further detected by inductively coupled plasma-atomic emission spectroscopy (ICP-AES) as shown in Table S1. Initially, Co<sub>0.85</sub>B<sub>0.15</sub>/NGH were prepared to test the catalytic activity toward the hydrolysis of AB. As expected, it needs more than 10 min to release only 2.5 equivalent of gas (Fig. 1a), with the TOF value of 6.2 min<sup>-1</sup>, which exhibits relatively low catalytic activity and hydrogen selectivity. However, after doping with the phosphorus, the resulted CoBP/NGH catalysts exhibit much enhanced catalytic activities with 100% hydrogen selectivity. Specifically, the Co<sub>0.79</sub>B<sub>0.15</sub>P<sub>0.06</sub>/NGH exhibited the highest catalytic activity among all the catalysts tested, with the TOF value of 32.8 min<sup>-1</sup>, which is almost 5 times higher than that of Co<sub>0.85</sub>B<sub>0.15</sub>/NGH without P doping, and higher than those of most of the previous reported non-noble metal based catalysts as shown in Table S2. These results highlight the synergistic effect between CoB and P in facilitating hydrolysis of AB. Furthermore, for comparison, the Co<sub>0.79</sub>B<sub>0.15</sub>P<sub>0.06</sub>/NGH NPs without supported material or supported on graphene oxide (GO) were also prepared, and their catalytic activities toward hydrolysis of AB were studied. As shown in Fig. S1, their catalytic activities are both inferior to that of Co<sub>0.79</sub>B<sub>0.15</sub>P<sub>0.06</sub>/NGH, suggesting the three dimensional nitrogen-doped graphene hydrogel is beneficial for the hydrolysis of AB (*vide infra*).

The durability of Co<sub>0.79</sub>B<sub>0.15</sub>P<sub>0.06</sub>/NGH was also tested in cycle experiment by adding the same molar amount of AB after the previous completion at room temperature. As shown in Fig. 1b, even after five cycles, the catalytic activity and hydrogen selectivity were still maintained well. To obtain the activation energy (E<sub>a</sub>) of catalytic hydrolysis of AB by Co<sub>0.79</sub>B<sub>0.15</sub>P<sub>0.06</sub>/NGH, the catalytic decomposition reaction temperatures were varied from 298 K to 313 K as shown in Fig. 2a. According to the Arrhenius equation, the

E<sub>a</sub> was calculated to be 39.42 kJ mol<sup>-1</sup>, which is quite lower than those of most of reported Co-based catalysts and even some noble-metal based catalysts as indicated in Table S2.

The powder X-ray diffraction (XRD) patterns of all the samples shown in Fig. S2 indicate the as-prepared CoBP/NGH catalysts with amorphous structure. It has been reported that amorphous structure belongs to metastable phase, which contains a lot of short-range order of atoms and long-range disorder structure with more active sites in comparison to the crystalline phase [53].

The Co<sub>0.79</sub>B<sub>0.15</sub>P<sub>0.06</sub> was also analyzed by X-ray photoelectron spectroscopy (XPS). As shown in Fig. 3a, the signals of Co 2p<sub>3/2</sub> peaks at binding energies of 778.5eV, 780.6eV and 786.4eV are assigned to the Co<sup>0</sup>, oxidized Co and satellite state, respectively. Similarly, the signals of P 2p peaks (Fig. 3b) at binding energies of 129.1eV and 133.5 eV are attributed to P<sup>0</sup> and oxidized P, respectively. And the signals of B 1s (Fig. 3c) peaks located at binding energies of 188.7eV and 191.7eV are attributed to B<sup>0</sup> and B–O, respectively. The formation of oxidized metals may be result from being exposure to oxygen during the catalysts preparation process [54]. Obviously, after doping P, the peak of Co 2p<sub>3/2</sub> located at the binding energies of 778.5eV has a positive shift of 0.4 eV in Co<sub>0.79</sub>B<sub>0.15</sub>P<sub>0.06</sub>/NGH when comparing to Co<sub>0.85</sub>B<sub>0.15</sub>/NGH, probably due to the decrease of electron density and increase of d-band vacancies in the metal active sites [55], which might result in boosting the catalytic activity. On the other hand, comparing with the binding energy of pure P (129.7eV) [56], the peaks of P 2p located at the binding energy of the 129.1eV for Co<sub>0.79</sub>B<sub>0.15</sub>P<sub>0.06</sub>/NGH is negative shifted to about 0.6 eV, which indicates that there is low charge transfer from the Co to P. In addition, the peaks of B 1s located at the binding energy of the 188.7 eV for Co<sub>0.79</sub>B<sub>0.15</sub>P<sub>0.06</sub>/NGH has a positive shifted of 0.3 eV comparing with the binding energy of pure B (188.4eV) [57]. All results indicate that there is strong electronic interaction between Co, P and B, which can further influence the bonding configuration of the metal active center, resulting in an enhancement of catalytic activity. Furthermore, as shown in Fig. S3, for the C1s of Co<sub>0.79</sub>B<sub>0.15</sub>P<sub>0.06</sub>/NGH, it can be seen clearly that the oxygen containing functional groups –C–O, and –C=O disappeared, and the –COO decreased significantly, comparing with the C1s of GO (Fig. S2a) [58], which suggest that the abundant of oxygen groups have been reduced. At the same time, a new peak at 285.2eV can be observed, which is due to the doping of nitrogen atoms. Meanwhile, as shown in Fig. S4, three types of nitrogen doped species can be observed clearly for N1s of Co<sub>0.79</sub>B<sub>0.15</sub>P<sub>0.06</sub>/NGH NPs. The binding energies of 399.6 eV, 398.1 eV and 400.8 eV are corresponding to pyrrolic N and pyridinic N, graphitic N, respectively [59]. In general, it can be suggested that nitrogen atom has been doped into the carbon bonds of graphene

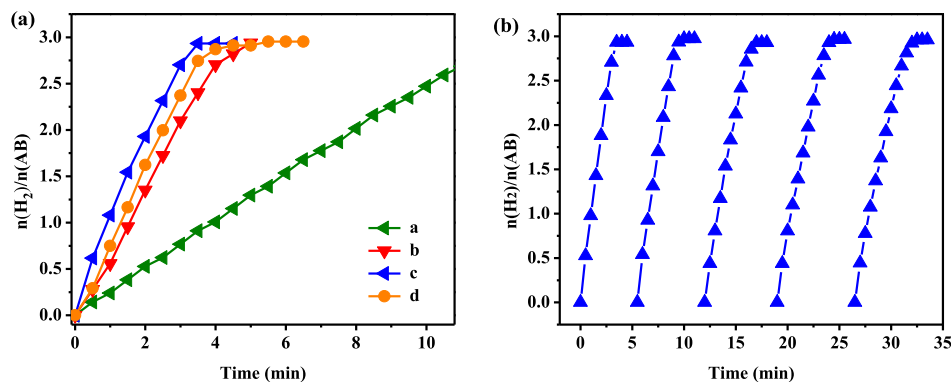
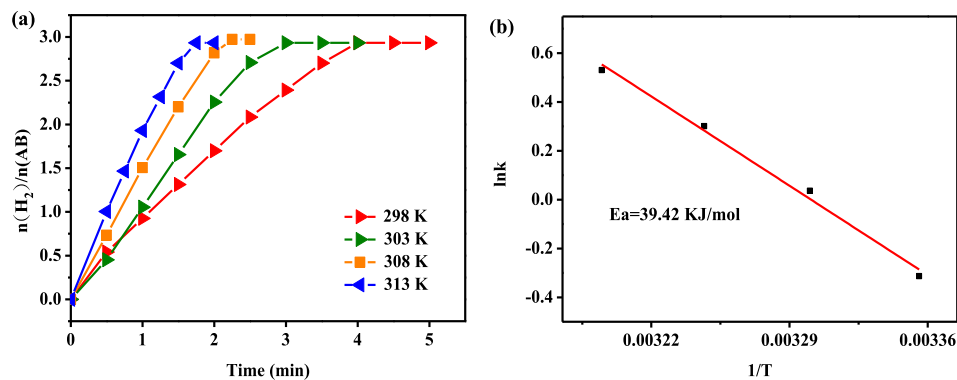
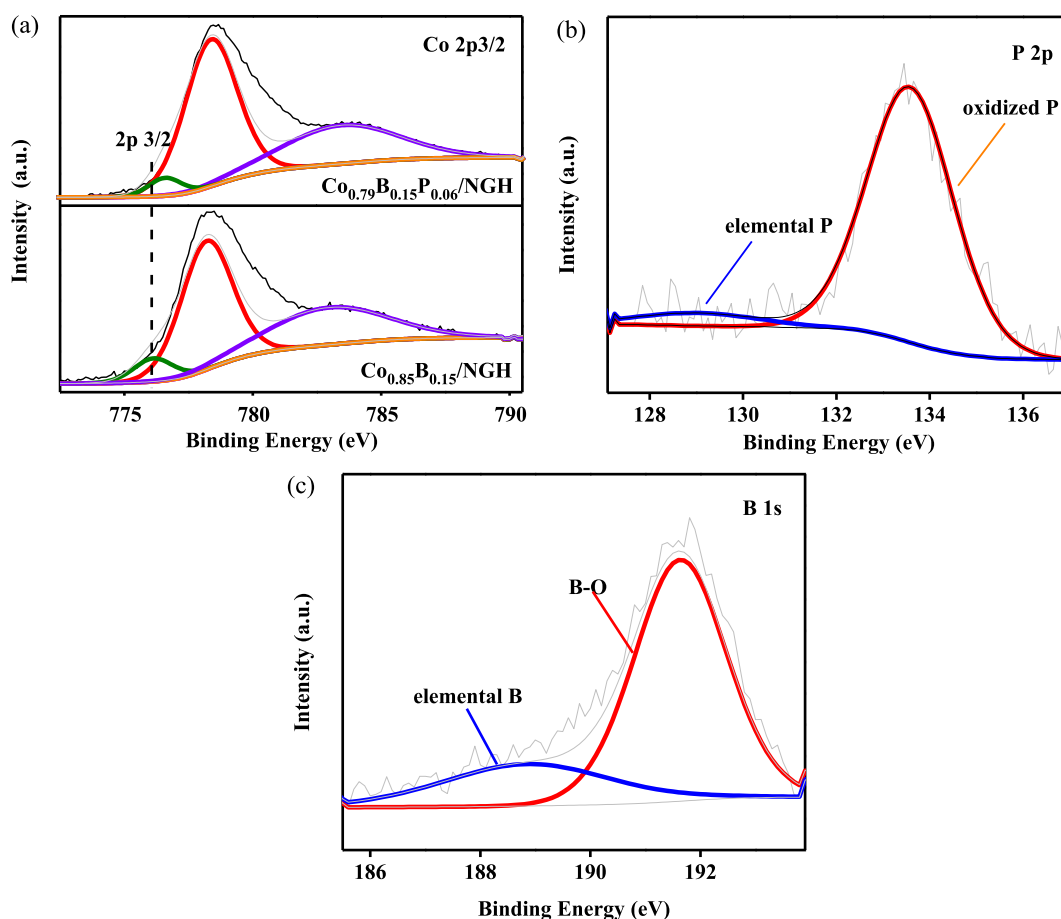


Fig. 1. (a) Catalytic performance tests of Co<sub>0.79</sub>B<sub>0.15</sub>P<sub>0.06</sub>/NGH with different molar of P content. (catalyst/NH<sub>3</sub>BH<sub>3</sub> = 0.04) (a, b, c, and d, represent the Co<sub>0.85</sub>B<sub>0.15</sub>/NGH, Co<sub>0.80</sub>B<sub>0.16</sub>P<sub>0.04</sub>/NGH, Co<sub>0.79</sub>B<sub>0.15</sub>P<sub>0.06</sub>/NGH, Co<sub>0.80</sub>B<sub>0.13</sub>P<sub>0.07</sub>/NGH) (b) durability tests of Co<sub>0.79</sub>B<sub>0.15</sub>P<sub>0.06</sub>/NGH toward the dehydrogenation hydrolysis of NH<sub>3</sub>BH<sub>3</sub> at room temperature.



**Fig. 2.** (a) Time plots for hydrogen generation toward the dehydrogenation hydrolysis of  $\text{NH}_3\text{BH}_3$  catalyzed by  $\text{Co}_{0.79}\text{B}_{0.15}\text{P}_{0.06}/\text{NGH}$  at temperatures ranging from 298 to 313 K. (catalyst/ $\text{NH}_3\text{BH}_3 = 0.04$ ) (b) Arrhenius plot of  $\ln k$  versus  $1/T$  during the hydrolysis of  $\text{NH}_3\text{BH}_3$  over  $\text{Co}_{0.79}\text{B}_{0.15}\text{P}_{0.06}/\text{NGH}$ .



**Fig. 3.** (a) The XPS spectra of (a) Co 2p 3/2 and (b) P 2p and (c) B 1s for the  $\text{Co}_{0.79}\text{B}_{0.15}\text{P}_{0.06}/\text{NGH}$  NPs.

successfully from the C 1s and N 1s of  $\text{Co}_{0.79}\text{B}_{0.15}\text{P}_{0.06}/\text{NGH}$  NPs, which may significantly enhance the interaction between metal and support to facilitate the hydrolysis of AB [60].

Furthermore, as shown in Fig. S5, the N-doped graphene hydrogel is cylindrical elastic hydrogel solid, with the diameter of 2.1 nm and height of 3.7 nm. It can be seen clearly from the scanning electron microscope (SEM) (Fig. S6), the structure of NGH is three-dimensional porous reticulate, which has varieties of porous sizes. Furthermore, the porosity of the NGH was measured by  $\text{N}_2$  adsorption/desorption at 77 K. As shown in Fig. S7(a), the BET specific surface area of the NGH sample is  $190.42 \text{ m}^2/\text{g}$ . From the

pore-size distribution of the NGH (Fig. S7(b)), it can be seen clearly that most of the pores possessing a volume of  $0.288 \text{ cm}^3/\text{g}$ , with a peak pore diameter of 3.697 nm. It is reported that these pores could greatly increase the contact with AB and facilitate the facile release or evolved hydrogen bubbles during the catalysis [61].

The microstructure of the obtained  $\text{Co}_{0.79}\text{B}_{0.15}\text{P}_{0.06}/\text{NGH}$  NPs were analyzed by transmission electron microscopy (TEM). As shown in Fig. 4a and b,  $\text{Co}_{0.79}\text{B}_{0.15}\text{P}_{0.06}$  nanoparticles are well dispersed on the 3D NGH. For comparison,  $\text{Co}_{0.85}\text{B}_{0.15}/\text{NGH}$  NPs were also characterized by TEM (Fig. S8), however, severely aggregation is observed, which might impede the mutual effect

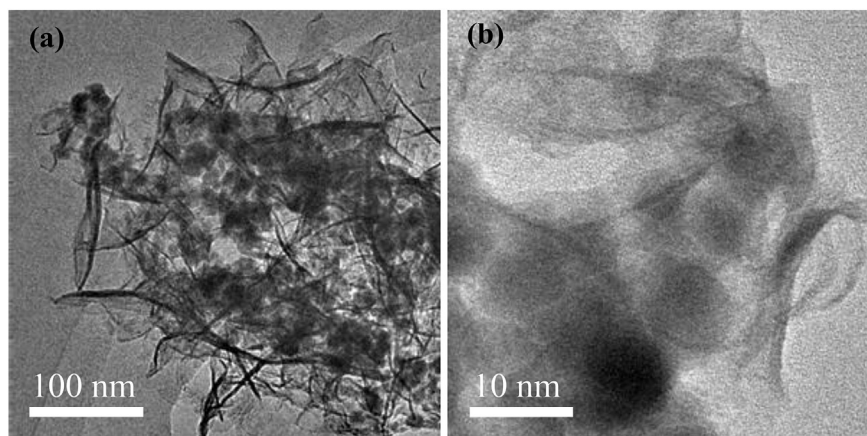


Fig. 4. TEM images of with different magnifications (a, b) of  $\text{Co}_{0.79}\text{B}_{0.15}\text{P}_{0.06}/\text{NGH}$ .

between the  $\text{NH}_3\text{BH}_3$  molecule and metal active centers, resulting in the decrease of the catalytic activity. Furthermore, the energy-dispersive X-ray (EDX), as shown in Fig. S9, confirms the co-presence of Co, B and P. In addition, the CoBP/NGH catalysts after stability test were further characterized by XRD and TEM. As shown in Fig. S10, the XRD indicates CoBP/NGH after stability test still possess amorphous structure. However, slight aggregation of CoBP NPs were observed from the TEM images as shown in Fig. S11, which might be the reason for the decrease of the catalytic performance. Further study about increasing the stability of the catalysts is still in process in our lab.

#### 4. Conclusions

In summary, the three-dimensional nitrogen doped graphene hydrogel (NGH) was obtained by a simple hydrothermal method, and further used as support to anchor CoBP NPs with good dispersion. Taking the advantage of P doping with resulted synergistic electronic interaction between Co, B, and P, as well as the strong metal-support interaction between CoBP and 3D NGH, the resulted  $\text{Co}_{0.79}\text{B}_{0.15}\text{P}_{0.06}/\text{NGH}$  catalyst exhibits superior catalytic performance toward the catalytic hydrolysis of  $\text{NH}_3\text{BH}_3$  at room temperature, with a TOF value of  $32.8 \text{ min}^{-1}$ , which is almost 5 times higher than that of undoped  $\text{Co}_{0.85}\text{B}_{0.15}/\text{NGH}$  NPs. This simple and low-cost synthetic method not only facilitate the promotion of ammonia borane as chemical hydrogen storage material but also open a new avenue for the fabrication of other bi- or multi-hetero atoms doped metal catalysts for more applications.

#### Acknowledgements

This work was financially supported by the National Natural Science Foundation of China (21571145), and Large-scale Instrument and Equipment Sharing Foundation of Wuhan University.

#### Appendix A. Supplementary data

Supplementary data related to this article can be found at <https://doi.org/10.1016/j.jallcom.2017.11.137>.

#### References

- [1] M.P. Suh, H.J. Park, T.K. Prasad, D.W. Lim, Hydrogen storage in metal-organic frameworks, *Chem. Rev.* 112 (2011) 782–835.
- [2] S. Dunn, Hydrogen futures: toward a sustainable energy system, *Int. J. Hydrogen Energy* 27 (2002) 235–264.
- [3] M. Pagliaro, A.G. Konstandopoulos, R. Ciriminna, G. Palmisano, Solar hydrogen: fuel of the near future, *Energy Environ. Sci.* 3 (2010) 279–287.
- [4] A. Boddien, D. Mellmann, F. Gärtner, R. Jackstell, H. Junge, P.J. Dyson, et al., Efficient dehydrogenation of formic acid using an iron catalyst, *Science* 333 (2011) 1733–1736.
- [5] R. Zeb, L. Salar, U. Awan, K. Zaman, M. Shahbaz, Causal links between renewable energy, environmental degradation and economic growth in selected SAARC countries: progress towards green economy, *Renew. Energy* 71 (2014) 123–132.
- [6] G. Cipriani, D.V. Di, F. Genduso, C.D. La, R. Liga, R. Miceli, et al., Perspective on hydrogen energy carrier and its automotive applications, *Int. J. Hydrogen Energy* 39 (2014) 8482–8494.
- [7] J. Graetz, New approaches to hydrogen storage, *Chem. Soc. Rev.* 38 (2009) 73–82.
- [8] W. Luo, P.G. Campbell, L.N. Zakharov, S.Y. Liu, A single-component liquid-phase hydrogen storage material, *J. Am. Chem. Soc.* 133 (2011) 19326–19329.
- [9] D. Pukazhselvan, V. Kumar, S. Singh, High capacity hydrogen storage: basic aspects, new developments and milestones, *Nano Energy* 1 (2012) 566–589.
- [10] W. Lei, H. Zhang, Y. Wu, B. Zhang, D. Liu, S. Qin, et al., Oxygen-doped boron nitride nanosheets with excellent performance in hydrogen storage, *Nano Energy* 6 (2014) 219–224.
- [11] E. Ha, L.Y.S. Lee, J. Wang, F. Li, K.Y. Wong, S.C.E. Tsang, Significant enhancement in photocatalytic reduction of water to hydrogen by  $\text{Au}/\text{Cu}_2\text{ZnSnS}_4$  nanostructure, *Adv. Mater.* 26 (2014) 3496–3500.
- [12] M.V. Lototskiy, V.A. Yartys, B.G. Pollet, R.C. Bowman, Metal hydride hydrogen compressors: a review, *Int. J. Hydrogen Energy* 39 (2014) 5818–5851.
- [13] S. Fukuzumi, T. Suenobu, Hydrogen storage and evolution catalysed by metal hydride complexes, *Dalton Trans.* 42 (2013) 18–28.
- [14] Q.L. Zhu, Q. Xu, Liquid organic and inorganic chemical hydrides for high-capacity hydrogen storage, *Energy Environ. Sci.* 8 (2015) 478–512.
- [15] M. Yadava, Q. Xu, Liquid-phase chemical hydrogen storage materials, *Energy Environ. Sci.* 5 (2012) 9698–9725.
- [16] D. Pukazhselvan, V. Kumar, S.K. Singh, High capacity hydrogen storage: basic aspects, new developments and milestones, *Nano Energy* 1 (2012) 566–589.
- [17] Q. Xu, M. Chandra, Catalytic activities of non-noble metals for hydrogen generation from aqueous ammonia-borane at room temperature, *J. Power Sources* 163 (2006) 364–370.
- [18] J.M. Yan, X.B. Zhang, S. Han, H. Shioyama, Q. Xu, Iron-nanoparticle-catalyzed hydrolytic dehydrogenation of ammonia borane for chemical hydrogen storage, *Angew. Chem. Int. Ed.* 47 (2008) 2287–2289.
- [19] L. Wen, J. Su, X. Wu, P. Cai, W. Luo, G.Z. Cheng, Ruthenium supported on MIL-96: an efficient catalyst for hydrolytic dehydrogenation of ammonia borane for chemical hydrogen storage, *Int. J. Hydrogen Energy* 39 (2014) 17129–17135.
- [20] Z.H. Lu, J. Li, A. Zhu, Q. Yao, W. Huang, R. Zhou, et al., Catalytic hydrolysis of ammonia borane via magnetically recyclable copper iron nanoparticles for chemical hydrogen storage, *Int. J. Hydrogen Energy* 38 (2013) 5330–5337.
- [21] S.K. Singh, Q. Xu, Bimetallic nickel-iridium nanocatalysts for hydrogen generation by decomposition of hydrous hydrazine, *Chem. Commun.* 46 (2010) 6545–6547.
- [22] S.K. Singh, Q. Xu, Bimetallic Ni–Pt nanocatalysts for selective decomposition of hydrazine in aqueous solution to hydrogen at room temperature for chemical hydrogen storage, *Inorg. Chem.* 49 (2010) 6148–6152.
- [23] S.K. Singh, Q. Xu, Complete conversion of hydrous hydrazine to hydrogen at room temperature for chemical hydrogen storage, *J. Am. Chem. Soc.* 131 (2009) 18032–18033.
- [24] J.M. Yan, Z.L. Wang, L. Gu, S.J. Li, H.L. Wang, W.T. Zheng, et al., AuPd–MnOx/MOF–graphene: an efficient catalyst for hydrogen production from formic acid at room temperature, *Adv. Energy Mater.* 5 (2015) 10–11.
- [25] L. Yang, W. Luo, G.Z. Cheng, Monodisperse CoAgPd nanoparticles assembled on graphene for efficient hydrogen generation from formic acid at room

- temperature, *Int. J. Hydrogen Energy* 41 (2016) 439–446.
- [26] M. Paladini, G.M. Arzac, V. Godinho, M.J. De Haro, A. Fernández, Supported Co catalysts prepared as thin films by magnetron sputtering for sodium borohydride and ammonia borane hydrolysis, *Appl. Catal. B Environ.* 158 (2014) 400–409.
- [27] W. Chen, J. Ji, X. Feng, X. Duan, G. Qian, P. Li, et al., Mechanistic insight into size-dependent activity and durability in Pt/CNT catalyzed hydrolytic dehydrogenation of ammonia borane, *J. Am. Chem. Soc.* 136 (2014) 16736–16739.
- [28] J.F. Shen, L. Yang, K. Hu, W. Luo, G.Z. Cheng, Rh nanoparticles supported on graphene as efficient catalyst for hydrolytic dehydrogenation of amine boranes for chemical hydrogen storage, *Int. J. Hydrogen Energy* 40 (2015) 1062–1070.
- [29] L. Wen, Z. Zheng, W. Luo, P. Cai, G.Z. Cheng, Ruthenium deposited on MCM-41 as efficient catalyst for hydrolytic dehydrogenation of ammonia borane and methylamine borane, *Chin. Chem. Lett.* 26 (2015) 1345–1350.
- [30] X.Q. Du, S.Y. Tan, P. Cai, W. Luo, G.Z. Cheng, A RhNiP/rGO hybrid for efficient catalytic hydrogen generation from an alkaline solution of hydrazine, *J. Mater. Chem. A* 4 (2016) 14572–14576.
- [31] Y.S. Du, N. Cao, L. Yang, W. Luo, G.Z. Cheng, One-step synthesis of magnetically recyclable rGO supported Cu@Co core-shell nanoparticles: highly efficient catalysts for hydrolytic dehydrogenation of ammonia borane and methylamine borane, *New J. Chem.* 37 (2013) 3035–3042.
- [32] W.Q. Feng, I. Yang, N. Cao, C. Du, H.M. Dai, L. Luo, G.Z. Cheng, In situ facile synthesis of bimetallic CoNi catalyst supported on graphene for hydrolytic dehydrogenation of amine borane, *Int. J. Hydrogen Energy* 39 (2014) 3371–3380.
- [33] Y. Xu, R. Wu, J. Zhang, Y. Shi, B. Zhang, Anion-exchange synthesis of nanoporous FeP nanosheets as electrocatalysts for hydrogen evolution reaction, *Chem. Commun.* 49 (2013) 6656–6658.
- [34] E.J. Popczun, J.R. McKone, C.G. Read, A.J. Bicchi, A.M. Wiltrout, N.S. Lewis, R.E. Schaak, Nanostructured nickel phosphide as an electrocatalyst for the hydrogen evolution reaction, *J. Am. Chem. Soc.* 135 (2013) 9267–9270.
- [35] J. Tian, Q. Liu, N. Cheng, A.M. Asiri, X. Sun, Self-Supported Cu<sub>3</sub>P Nanowire Arrays as an integrated high-performance three-dimensional cathode for generating hydrogen from water, *Angew. Chem. Int. Ed.* 53 (2014) 9577–9581.
- [36] X. Yang, A.Y. Lu, Y. Zhu, M.N. Hedhili, S. Min, K.W. Huang, Y. Han, L.J. Li, CoP nanosheet assembly grown on carbon cloth: a highly efficient electrocatalyst for hydrogen generation, *Nano Energy* 15 (2015) 634–641.
- [37] A. Berenguer, T.M. Sankaranarayanan, G. Gómez, I. Moreno, J.M. Coronado, P. Pizarro, et al., Evaluation of transition metal phosphides supported on ordered mesoporous materials as catalysts for phenol hydrodeoxygenation, *Green Chem.* 18 (2016) 1938–1951.
- [38] Z. Huang, Z. Chen, Z. Chen, C. Lv, M.G. Humphrey, C. Zhang, Cobalt phosphide nanorods as an efficient electrocatalyst for the hydrogen evolution reaction, *Nano Energy* 9 (2014) 373–382.
- [39] Y. Shi, B. Zhang, Recent advances in transition metal phosphide nanomaterials: synthesis and applications in hydrogen evolution reaction, *Chem. Soc. Rev.* 45 (2016) 1529–1541.
- [40] H. Yan, C. Tian, L. Wang, A. Wu, M. Meng, L. Zhao, H. Fu, Modified tungsten Nitride/Reduced graphene oxide as a high-performance, non-noble-metal electrocatalyst for the hydrogen evolution reaction, *Angew. Chem. Int. Ed.* 127 (2015) 6423–6427.
- [41] P. Xiao, M.A. Sk, L. Thia, X. Ge, R.J. Lim, J. Wang, K.H. Lima, X. Wang, Nanostructured PtRu/C catalyst promoted by CoP as an efficient and robust anode catalyst in direct methanol fuel cells, *Energy Environ. Sci.* 7 (2014) 2624–2629.
- [42] C.Y. Peng, K. Kang, S. Cao, Y. Chen, Z.S. Lin, W.F. Fu, Nanostructured Ni<sub>2</sub>P as a robust catalyst for the hydrolytic dehydrogenation of ammonia-borane, *Angew. Chem. Int. Ed.* 127 (2015) 15951–15955.
- [43] Z.C. Fu, Y. Xu, S.L.F. Chan, W.W. Wang, F. Li, F. Lang, Highly efficient hydrolysis of ammonia borane by anion (–OH, F–, Cl–)-tuned interactions between reactant molecules and CoP nanoparticles, *Chem. Commun.* 53 (2017) 705–708.
- [44] J. Yan, J. Liao, H. Li, H. Wang, R.F. Wang, Magnetic field induced synthesis of amorphous CoB alloy nanowires as a highly active catalyst for hydrogen generation from ammonia borane, *Catal. Commun.* 84 (2016) 124–128.
- [45] A.K. Figen, Dehydrogenation characteristics of ammonia borane via boron-based catalysts (Co–B, Ni–B, Cu–B) under different hydrolysis conditions, *Int. J. Hydrogen Energy* 38 (2013) 9186–9197.
- [46] Y.J. Zou, Y.B. Gao, C.L. Xiang, H.L. Chu, S.J. Qiu, E.H. Yan, et al., Cobalt-Nickel-boron supported over polypyrrole-derived activated carbon for hydrolysis of ammonia borane, *Metals* 6 (2016) 154.
- [47] Y. Xu, K. Sheng, C. Li, G. Shi, Self-assembled graphene hydrogel via a one-step hydrothermal process, *ACS Nano* 4 (2010) 4324–4330.
- [48] Z. Zhao, T. Mei, Y. Chen, J. Qiu, D. Xu, J. Wang, et al., One-pot synthesis of lightweight nitrogen-doped graphene hydrogels with supercapacitive properties, *Mater. Res. Bull.* 68 (2015) 245–253.
- [49] Y. Xu, Z. Lin, X. Huang, Y. Liu, Y. Huang, X. Duan, Flexible solid-state supercapacitors based on three-dimensional graphene hydrogel films, *ACS Nano* 7 (2013) 4042–4049.
- [50] Y. Li, Y. Zhao, H. Cheng, Y. Hu, G. Shi, L. Dai, et al., Nitrogen-doped graphene quantum dots with oxygen-rich functional groups, *J. Am. Chem. Soc.* 134 (2011) 15–18.
- [51] D.C. Marcano, D.V. Kosynkin, J.M. Berlin, A. Sinititskii, Z. Sun, A. Slesarev, et al., Improved synthesis of graphene oxide, *ACS Nano* 4 (2010) 4806–4814.
- [52] X.Q. Du, C. Liu, C. Du, P. Cai, G.Z. Cheng, W. Luo, Nitrogen-doped graphene hydrogel-supported NiPt–CeO<sub>x</sub> nanocomposites and their superior catalysis for hydrogen generation from hydrazine at room temperature, *Nano Res.* 10 (2017) 2856–2865.
- [53] Y. Ma, H. Li, H. Wang, X. Mao, V. Linkov, S. Ji, et al., Evolution of the electrocatalytic activity of carbon-supported amorphous platinum-ruthenium-nickel-phosphorous nanoparticles for methanol oxidation, *J. Power Sources* 268 (2014) 498–507.
- [54] N. Cao, L. Yang, C. Du, J. Su, W. Luo, G. Cheng, Highly efficient dehydrogenation of hydrazine over graphene supported flower-like Ni–Pt nanoclusters at room temperature, *J. Mater. Chem. A* 2 (2014) 14344–14347.
- [55] X.Q. Du, S.Y. Tan, P. Cai, W. Luo, G.Z. Cheng, A RhNiP/rGO hybrid for efficient catalytic hydrogen generation from an alkaline solution of hydrazine, *J. Mater. Chem. A* 4 (2016) 14572–14576.
- [56] V.D. Klimov, A.A. Vashman, I.S. Pronin, Study of atomic titanium interaction with PF<sub>3</sub> matrix at 77-K-cryochemical synthesis of TiF<sub>2</sub>, PF<sub>3</sub> mono-tri-phosphinitanium (II) fluoride new compounds, *Zhurnal Obshchei Khimii* 61 (1991) 2166–2174.
- [57] L. Chen, T. Goto, T. Hirai, Amano, State of boron in chemical vapour-deposited SiC-B composite powders, *J. Mater. Sci. Lett.* 9 (1990) 997–999.
- [58] D.X. Yang, A. Velamakanni, G. Bozoklu, S. Park, M. Stoller, R.D. Piner, S. Stankovich, I. Jung, D.A. Field, Chemical analysis of graphene oxide films after heat and chemical treatments by X-ray photoelectron and micro-Raman spectroscopy, *Carbon* 47 (2009) 145–152.
- [59] P. Chen, J.J. Yang, S.S. Li, Z. Wang, T.Y. Xiao, Y.H. Qian, et al., Hydrothermal synthesis of macroscopic nitrogen-doped graphene hydrogels for ultrafast supercapacitor, *Nano Energy* 2 (2013) 249–256.
- [60] J.J. Zhang, R.Y. Li, Z.J. Li, J.K. Liu, Z.G. Gu, G.L. Wang, Synthesis of nitrogen-doped activated graphene aerogel/gold nanoparticles and its application for electrochemical detection of hydroquinone and o-dihydroxybenzene, *Nanoscale* 10 (2014) 5458–5466.
- [61] X.P. Zhang, D. Liu, L. Yang, L.M. Zhou, T.Y. You, Self-assembled three-dimensional graphene-based materials for dye adsorption and catalysis, *J. Mater. Chem. A* 3 (2015) 10031–10037.